JOURNAL OF VIROLOGY, Dec. 2004, p. 13285–13292 Vol. 78, No. 23
0022-538X/04/$08.00+0 DOI: 10.1128/JVI.78.23.13285–13292.2004

Structural Requirements of Astrovirus Virus-Like Particles Assembled in Insect Cells

Santiago Caballero,[1] Susana Guix,[1] Enric Ribes,[2] Albert Bosch,[1]* and Rosa M. Pintó[1]

Enteric Virus Group, Department of Microbiology,[1] and Department of Cell Biology,[2] School of Biology, University of Barcelona, Barcelona, Spain

Received 31 March 2004/Accepted 23 July 2004

Expression of the complete ORF2 of human astrovirus serotype 1 (HAstV-1) in the baculovirus system led to the formation of virus-like particles (VLPs) of around 38 nm. The same kind of VLPs were also obtained either with the expression of a truncated form of ORF2 lacking the first 70 amino acids (aa), or with the same truncated form in which those 70 aa were replaced by the green fluorescent protein. All three kinds of VLPs were equally recognized by an anti-HAstV-1 polyclonal antibody and by two monoclonal antibodies (MAbs; 8E7 and 5B7), indicating a nonessential role of those amino acids neither in the capsid assembly nor in the antigen structure. A second type of structure consisting of 16-nm ring-like units was observed in all of the cases, mostly after disassembling the 38-nm VLPs through the addition of EDTA. The removal of the EDTA and the addition of Mg^{2+} ions promoted the reassembly of the 38-nm VLPs. The nature of these 16-nm ring-like structures, capsomers or T = 1 VLPs, still remains unclear. Biochemical analysis revealed no differences between the 38-nm VLPs and the 16-nm structures, whereas antigenically, they shared the 8E7 MAb epitope but differed in the 5B7 MAb epitope, with the latter structures being more readily recognized.

Human astroviruses (HAstV) are a frequent causal agent of gastroenteritis in children worldwide (5, 10, 12, 14, 24, 27, 28, 35, 38), although they have also been associated with the elderly (4, 29, 34). Eight serotypes have been described, with serotype 1 (HAstV-1) being the most globally prevalent (12, 14, 18, 27, 28, 33, 36). Astroviruses are nonenveloped viruses whose capsid is around 28 to 41 nm in diameter and contains a plus-sense single-stranded RNA of around 6.9 kb organized in three open reading frames (ORFs) (20, 32, 37). ORF1a and ORF1b encode the nonstructural proteins (19, 21, 22), whereas ORF2 encodes the structural proteins through a subgenomic RNA (25). ORF2 of HAstV-1 encodes a polyprotein of 787 amino acids (aa) in length, with a molecular mass of around 87 kDa (26), which is the precursor of the smaller 24- to 26-kDa, 29- to 31-kDa, and 32- to 34-kDa structural proteins (1, 3, 26). The proteolytical processing from the precursor to the mature structural proteins is still very controversial, and to date, three different models have been proposed (1, 13, 23). In the first model, Bass and Qiu (1) proposed an intracellular processing of the precursor polyprotein at the amino terminus between residues 70(R) and 71(K) before capsid assembly, with this capsid being further processed extracellularly by the action of trypsin and giving the above-mentioned mature proteins. In subsequent studies, the intracellular processing of this model was refused (13), with the complete precursor being the assembly unit. Later on, Méndez and colleagues (23) proposed a third model in which the structural precursor of HAstV-8 is intracellularly processed at the carboxy terminus prior to its assembly into the capsid, although the cleavage site has not yet been identified.

The expression of the genomes encoding the capsid proteins of a great number of RNA viruses giving rise to the formation of virus-like particles (VLPs) has been accomplished in different heterologous expression systems, including the expression of the complete ORF2 of HAstV-2 in the vaccinia system (8). In the present study, the assembly of VLPs into the baculovirus expression system from either the complete ORF2 or a 5′-truncated construct starting at residue 71 of HAstV-1 is described, as is the addition of the green fluorescence protein (GFP) to the truncated polyprotein.

MATERIALS AND METHODS

Cells and viruses. *Sf*9 cells were grown at 28°C in TC100 medium containing 10% heat inactivated fetal calf serum (FCS) and 100,000 IU of penicillin and 100,000 μg of streptomycin per liter. Virus stocks of a polyhedrin-negative baculovirus strain (AcNPVRP8; kindly provided by R. D. Possee, NERC Institute of Virlogy, Oxford, England) and of HAstV-1 recombinant strains were prepared by infecting *Sf*9 cells at a multiplicity of infection (MOI) of 0.1 and allowing the infection to proceed for 5 to 7 days. Viruses were harvested from the culture medium by centrifugation at 1,000 × *g*, and the cell debris was discarded. Viruses were titrated by plaque assays and stored at 4°C.

CaCo-2 cells were grown at 37°C in minimal essential medium containing 10% FCS, 100,000 IU of penicillin and 100,000 μg of streptomycin per liter, 0.15% (wt/vol) sodium bicarbonate, 15 mM HEPES, 2 mM glutamine, and nonessential amino acids. A cell-adapted strain of HAstV-1 (kindly provided by M. Koopmans, RIVM, Bilthoven, The Netherlands) was propagated in CaCo-2 cells, as previously described (30). Prior to inoculation, viruses were preactivated through a trypsin treatment at a final concentration of 10 μg/ml for 30 min at 37°C. Additionally, trypsin at a concentration of 5 μg/ml was added in a serum-free overlay medium. Viral suspensions were released from the cell fraction at 72 h postinfection by lysing the cells in TN buffer (50 mM Tris-HCl [pH 7.4], 100 mM NaCl) in the presence of 1% NP-40.

Construction of HAstV-1 recombinant baculoviruses. Three transfer vectors containing the full-length ORF2 gene, a 5′-truncated ORF2 gene (ΔORF2, deletion of aa 1 to 70), and a fusion between the GFP gene of the jellyfish *Aequorea victoria* and ΔORF2 were generated by inserting PCR-amplified fragments flanked by NotI and PstI restriction enzyme sites in the pFastBac (Invitrogen) vector. The template used for the amplification of astrovirus sequences was the plasmid pAVIC6 (kindly provided by S. Matsui, Gastroenterology Section, Veterans Administration Palo Alto Health Care System, Palo Alto, Calif.), which contains the full genome of HAstV-1, and the plasmid pEGFP-1 (BD Biosciences) was used to amplify the GFP gene.

* Corresponding author. Mailing address: Department of Microbiology, University of Barcelona, Diagonal 645, 08028 Barcelona, Spain. Phone: 34 93 4034620. Fax: 34 93 4034629. E-mail: abosch@ub.edu.

The ORF2 gene, spanning from nucleotides 4328 to 6691, was amplified by using primers A4328 (5′-AGGAC**GCGGCCGC**CACCATGGCTAGCAAGTCC AATAAGC-3′), which contains a NotI restriction site (boldface type) and the Kozak's sequence (underlined), and A6691 (5′-TACCC**TGCAG**CTACTCGG CGTGGCCGCGGCT-3′), which contains a PstI restriction site (boldface type). The ΔORF2 gene, spanning from nucleotides 4538 to 6691, was amplified by using primers A4538 (5′-ACATT**GCGGCCGC**CACCATGGGTAAACAGGGT GTCACAGGACCAAAACC-3′), which also contains a NotI restriction site and the Kozak's sequence, and A6691. Amplification was performed with a 50 nM concentration of each primer and 0.5 IU of the *Pwo* polymerase (Roche). The PCR products were purified and digested with the NotI and PstI restriction enzymes for 1 h at 37°C. Digested products were purified from agarose gels and ligated into the pFastBac vector.

The fusion of the GFP-encoding and ΔORF2 DNAs was achieved through the ligation of their corresponding amplimers. The GFP gene was amplified by using primers NtGFP (5′-CGCTA**GCGGCCGC**CACCATGGTGAGCAAGGGCGA GGAGC-3′), which contains a NotI restriction site (boldface type) and the Kozak's sequence (underlined), and CtGFP (5′-GGATCC**TCTAGA**CATGTGG TGGTGGTGGTGGT-3′), which contains an XbaI restriction site (boldface type). The ΔORF2 gene was amplified by using primers NtΔORF2 (5′-TCAAT **TCTAGA**GGATCCAAACAGGGTGTCACAGGACCAA-3′), which contains an XbaI restriction site (boldface type) and a flexible linker (underlined) encoding the amino acids SRGS, and A6691. Both amplimers were digested with the XbaI restriction enzyme, purified, and ligated. The ligation product was digested with the NotI and PstI restriction enzymes for 1 h at 37°C and cloned into the pFastBac vector.

Recombinant baculoviruses were generated by using the Bac-to-Bac expression system (Invitrogen). Briefly, DH10Bac competent cells, which contain bacmid DNA, were transformed with the recombinant pFastBac transfer vectors. Colonies containing recombinant bacmids were identified by disruption of the *lacZ*α gene. High-molecular-weight DNA minipreps were prepared from selected colonies, and the released DNA was used to transfect *Sf*9 cells with Cellfectin (Invitrogen) to obtain the recombinant baculoviruses. Recombinant baculoviruses, i.e., AcNPV-ORF2, AcNPV-ΔORF2, and AcNPV-GFPΔORF2, were collected from the supernatants of transfected cells and stored at 4°C.

Recombinant protein synthesis. Heterologous protein synthesis was evaluated either in the cell fraction or in the supernatant of infected *Sf*9 cultures. In the first case, 1.2×10^7 *Sf*9 cells were seeded in an 80-cm^2 flask, infected at a MOI of 5 to 10 with either AcNPV-ORF2, AcNPV-ΔORF2, AcNPV-GFPΔORF2, or AcNPVRP8, and incubated at 28°C in TC100 medium supplemented with 1% FCS and a daily dose of 0.5 μg of the protease inhibitors aprotinin and leupeptin/ml. At 72 h postinfection, cells were harvested by centrifugation ($1,000 \times g$ for 10 min), resuspended in 1 ml of lysis buffer (TN buffer with 2% NP-40), and incubated at 4°C for 1 h and 30 min. Cell lysates were then centrifuged at $14,000 \times g$ for 5 min at 4°C. Supernatants and pellets, which represented soluble and nonsoluble fractions, respectively, were separated and analyzed by sodium dodecyl sulfate-polyacrylamide gel electrophoresis (SDS-PAGE) and Western blotting. In the second case, 1.2×10^8 *Sf*9 cells were infected at a MOI of 5 and incubated for 7 days in 72 ml of the same medium mentioned above. Cultures were centrifuged at $22,000 \times g$ for 30 min, and the supernatant was concentrated through a 35% sucrose cushion. The resulting pellet was resuspended in 1 ml of TN buffer and analyzed by SDS-PAGE and Western blotting.

Immunoblotting analysis. Samples were boiled in Laemmli buffer (1 M Tris-HCl [pH 6.8], 40% glycerol, 25% β-mercaptoethanol, 1% SDS, and 0.05% bromophenol blue), electrophoresed in an SDS–12% polyacrylamide gel, and blotted onto a nitrocellulose membrane. After blocking with 5% skim milk–TBS buffer (50 mM Tris-HCl [pH 7.6] and 100 mM NaCl), membranes were probed with a rabbit polyclonal anti-HAstV-1 antibody (kindly provided by Dorsey Bass, Division of Pediatric Gastroenterology, Stanford University, Calif.) and revealed with a secondary anti-rabbit immunoglobulin G (IgG) alkaline phosphatase-conjugated antibody (Sigma Aldrich). The enzyme reaction was developed by adding 5-bromo-4-chloro-3-indolylphosphate (BCIP) and nitroblue tetrazolium substrates.

Immunofluorescence and fluorescence analysis. Around 2×10^5 *Sf*9 cells were seeded onto coverslips in 24-well plates and infected at an MOI of 0.1 with the recombinant baculoviruses. Three days later, cells were washed with phosphate-buffered saline (PBS) buffer (140 mM NaCl, 27 mM KCl, 81 mM Na_2HPO_4, 15 mM KH_2PO_4 [pH 7.2]) and fixed with 3% paraformaldehyde for 30 min at room temperature. Cells infected with the AcNPV-ORF2 and AcNPV-ΔORF2 baculoviruses were further processed for the immunological detection of recombinant proteins, and cells infected with the AcNPV-GFPΔORF2 virus were directly observed for fluorescence. In both cases, cells infected with the AcNPVRP8 baculovirus were used as negative controls. For immunofluorescence, cells were permeabilized through a 15-min treatment with 0.5% Triton X-100 in 20 mM glycine–PBS buffer and blocked for 30 min with a 10% FCS solution in 20 mM glycine–PBS buffer. Cells were immunolabeled either with a rabbit polyclonal anti-HAstV-1 antibody or the 8E7 monoclonal antibody (MAb) (kindly provided by J. E. Herrmann, Department of Medicine and Infectious Diseases, University of Massachusetts Medical School, Worcester, Mass.) for 1 h. Bound antibodies were detected by a 1-h incubation with a fluorescein isothiocyanate-conjugated anti-rabbit IgG antibody or a fluorescein isothiocyanate-conjugate anti-mouse IgG antibody, respectively. Finally, cells were stained with 1 μg of 4′,6′-diamidino-2-phenylindole (DAPI)/ml in PBS for 15 min to locate the nucleus and mounted with Fluoromont G before observation under an epifluorescence microscope at a magnification of ×200. Images were captured with a digital camera with the Metamorph software. In the case of direct detection of GFP-associated fluorescence, cells were stained with DAPI as described above.

Purification of HAstV-1 and astrovirus VLPs in sucrose and CsCl gradients. One-milliliter samples of astrovirus stocks, soluble fractions from infected *Sf*9 cell extracts, and concentrates of infected cell supernatants were loaded on the top of either preformed 0 to 45% (wt/wt) 9-ml sucrose gradients or preformed 0 to 50% (wt/wt) 9-ml CsCl gradients in TN buffer. Sucrose gradients were centrifuged for 2 h and 45 min at $200,000 \times g$, and CsCl gradients were centrifuged for 18 h at $150,000 \times g$ as previously described (6). Gradients were fractionated, and the density for each fraction was estimated from the refraction index. Additionally, the presence of astrovirus antigens was analyzed through a sandwich enzyme-linked immunosorbent assay (ELISA).

ELISA. Astrovirus antigens were captured with either the 8E7 or 5B7 MAb and detected by using a rabbit polyclonal anti-HAstV-1 antibody. Specifically bound antibodies were revealed by a peroxidase-conjugated anti-rabbit IgG antibody (Sigma Aldrich).

Electron microscopy. Immunoreactive fractions corresponding to the different antigenic peaks were separately pooled and dialyzed against TN buffer. The presence and morphology of the astrovirus VLPs and HAstV-1 in the antigenic peaks were evaluated by transmission electron microscopy of negatively stained preparations. A 10-μl sample was applied to a 1% agarose block, and a carbon-coated 400-mesh copper grid was set on the drop for 30 min. Samples were negatively stained with 2% phosphotungstic acid at pH 6.4. Finally, the grids were examined in a Hitachi H 600 AB electron microscope.

To confirm the astroviral nature of the recombinant products, either an immunoaggregation or an immunogold labeling was performed by using the rabbit polyclonal anti-HAstV-1 antibody. In the first case, samples were incubated with the antibody for 1 h and subsequently adsorbed to carbon-coated copper grids. The presence of aggregates was indicative of a positive reaction. In the immunogold labeling, samples were adsorbed to grids as above described, blocked with 1% bovine serum albumin and 0.1% Tween 20–PBS for 15 min, incubated with the polyclonal anti-HAstV-1 antibody for 1 h, and finally, after thoroughly washing, incubated for 1 h with a rabbit IgG antibody conjugated to 10-nm colloidal gold particles. All samples were finally stained and observed as described above.

Disassembly and reassembly of VLPs. Purification in CsCl gradients of the different recombinant products and of HAstV-1 was performed as described above, except with TNE buffer (50 mM Tris-HCl [pH 7.4], 100 mM NaCl, 10 mM EDTA) to destabilize the VLPs by the addition of the chelating agent EDTA. The reassembly of the subviral structures into VLPs was tested by the removal of EDTA and the addition of Mg^{2+} through a 24-h dialysis at 4°C in front of TNMg buffer (50 mM Tris-HCl [pH 7.4], 100 mM NaCl, 10 mM $MgCl_2$). The identification of subviral and viral structures was determined by electron microscopy after dialyzing against the corresponding buffers. Proteolytic processing with trypsin (10 μg/ml, grade IX; Sigma) for 30 min at 37°C was performed on purified VLPs and rings.

Immunoprecipitation. To concentrate the subviral and viral purified structures, 800-μl samples of each type of structure were immunoprecipitated overnight at 4°C with the rabbit polyclonal anti-HAstV-1 antibody. The immune complexes were harvested by the addition of protein A-agarose and incubation at 4°C for 3 h, followed by centrifugation at $10,000 \times g$ for 1 min. Pellets were washed twice with TNE–0.1% NP-40 or TN–0.1% NP-40 for subviral or viral structures, respectively, and finally resuspended in 20 μl of the same buffer. Samples were disrupted by adding 5 μl of Laemmli buffer and boiling for 10 min, and the proteins were resolved by SDS-PAGE and Western blot as described above.

RESULTS

Analysis of recombinant proteins. The expression of the astrovirus genes in insect cells was first evaluated by in situ immunofluorescence and fluorescence. Expressed proteins

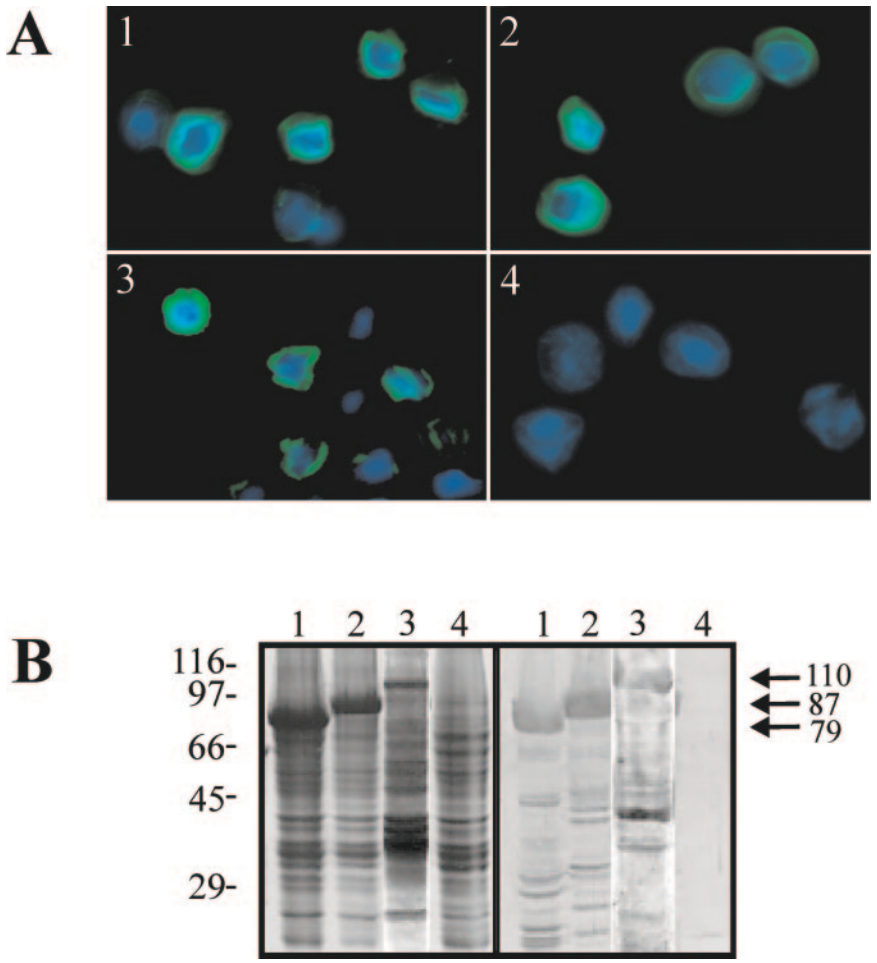

FIG. 1. (A) Fluorescence microscopy analysis of *Sf*9 cells infected with astrovirus recombinant baculoviruses. Immunofluorescence of cells infected with AcNPV-ΔORF2 (panel 1), AcNPV-ORF2 (panel 2), and AcNPVRP8 (panel 4) with MAb 8E7 is shown. The GFP fluorescence of AcNPV-GFPΔORF2-infected cells is also shown (panel 3). (B) SDS-polyacrylamide gel (left) and Western blot (right) analysis of total cell extracts of cells infected with AcNPV-ΔORF2 (lanes 1), AcNPV-ORF2 (lanes 2), AcNPV-GFPΔORF2 (lanes 3), and AcNPVRP8 (lanes 4). Arrows indicate the molecular mass (in kilodaltons) of each of the recombinant products. The immunological detection was performed with a polyclonal anti-HAstV-1 antibody.

were exclusively located in the cytoplasm of infected cells for the three recombinants, as could be observed through immunofluorescence of cells infected with either the AcNPV-ORF2 or AcNPV-ΔORF2 baculovirus or through a direct fluorescence analysis of cells infected with the AcNPV-GFPΔORF2 baculovirus (Fig. 1A). The immunofluorescence pattern was identical with both antibodies tested (data not shown).

To further evaluate the recombinant protein synthesis, SDS-PAGE and Western blot analyses of cell extracts and cell culture supernatants were performed. Immunologically specific protein bands of the expected sizes were detected in both cells and culture medium, with molecular masses of 87, 79, and 110 kDa for AcNPV-ORF2, AcNPV-ΔORF2, and AcNPV-GFPΔORF2, respectively (Fig. 1B). Regarding the cells, the expressed proteins were mainly detected in the nonsoluble fraction. Different mild detergents (2% NP-40, 2% Triton X-100, and 2% Tween 20) were used in an attempt to release the recombinant proteins from the membranes, but even after the treatments, most of the expressed proteins remained associated with the nonsoluble fraction, indicating a tight association with membranes (data not shown).

Expression of either complete ORF2, truncated ORF2, or truncated GFPΔORF2 leads to the formation of VLPs. To establish whether any of the recombinant products assembled into viral or subviral structures, they were purified in sucrose gradients. The soluble fraction obtained after lysing the infected cells was selected for the purification in spite of its lower recombinant protein content, since its manipulation was more reliable. Sucrose separation of the soluble fractions of infected cells revealed three antigenic peaks with densities of around 1.05, 1.08, and 1.12 g/ml (Fig. 2A), for all three recombinant baculoviruses. Concentrates of culture medium from infected cultures were also purified, and interestingly, only the 1.12-g/ml antigenic peak was detected (Fig. 2C). Under the same conditions, HAstV-1 suspensions were separated into three antigenic peaks with densities of 1.05, 1.12, and 1.14 g/ml (Fig. 2E), corresponding to soluble proteins, empty capsids, and infectious viruses, respectively (6).

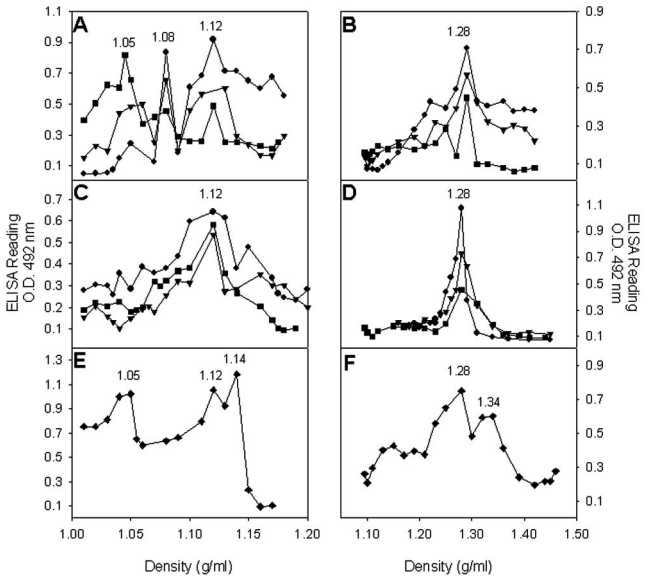

FIG. 2. Soluble fractions obtained after cell lysis (A and B) or culture medium concentrates (C and D) from recombinant baculovirus-infected *Sf*9 cells were fractionated on 0 to 45% sucrose gradients in TN buffer (A and C) or on 0 to 50% CsCl gradients in TN buffer (B and D). Gradient fractions were collected from the bottoms of the tubes and analyzed by a sandwich ELISA with MAb 8E7 as the astrovirus-capturing antibody and a polyclonal anti-HastV-1 as the detecting antibody. HAstV-1 stocks were fractionated in either 0 to 45% sucrose gradients in TN buffer (E) or 0 to 50% CsCl gradients in TN buffer (F) and used as controls. Refraction indices of each fraction were measured and transformed into density values. Circles, AcNPV-ORF2; triangles, AcNPV-ΔORF2; squares, AcNPV-GFPΔORF2; O.D., optical density.

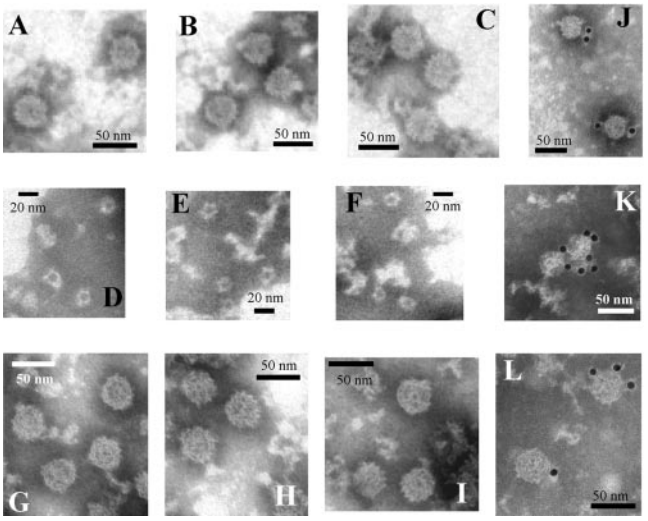

FIG. 3. Electron microscopy of recombinant astrovirus products. Negatively stained preparations of the 1.12-g/ml sucrose fractions from *Sf*9 cultures infected with AcNPV-ORF2 (A), AcNPV-ΔORF2 (B), and AcNPV-GFPΔORF2 (C) are shown. Negatively stained preparations of the 1.08-g/ml sucrose fractions from *Sf*9 cultures infected with AcNPV-ORF2 (D), AcNPV-ΔORF2 (E), and AcNPV-GFPΔORF2 (F) are shown. Negatively stained preparations of the 1.28-g/ml CsCl fractions from *Sf*9 cultures infected with AcNPV-ORF2 (G), AcNPV-ΔORF2 (H), and AcNPV-GFPΔORF2 (I) are shown. Immunogold labeling of the 1.12-g/ml fraction from the AcNPV-ORF2-infected *Sf*9 cultures (J, K, and L) is also shown.

Additionally, the same kind of samples were isopycnically separated in CsCl gradients. Soluble fractions as well as culture medium concentrates resolved into a single discrete antigenic peak of 1.28 g/ml for all of the recombinant products (Fig. 2B and D), and two antigenic peaks of 1.28 and 1.34 g/ml appeared with HAstV-1 suspensions (Fig. 2F), corresponding to empty capsids and infectious viruses, respectively (40).

Recombinant antigenic peaks corresponding to empty particles (1.12 and 1.28 g/ml in the sucrose and CsCl gradients, respectively) were analyzed by electron microscopy. In all cases, VLPs of around 38 nm in diameter were observed (Fig. 3). To confirm the nature of the VLPs, a gold labeling technique with specific antibodies was performed and gold-decorated VLPs could be observed in all cases and those corresponding to AcNPV-ORF2 are shown in Fig. 3.

To know the nature of the newly identified sucrose antigenic peaks (1.05 and 1.08 g/ml), an electron microscopy study was again carried out. The 1.05-g/ml peak was void of any type of structure while the peak of 1.08 g/ml contained mainly the same kind of 38-nm VLPs seen in the 1.12-g/ml peak, although in lesser amounts, and a few of the ring-like structures of 16 nm (Fig. 3). The presence of two different kind of structures in the 1.08-g/ml peak could be interpreted as cross-contamination between fractions or as a tendency of one type of structure to give rise to the other. To further characterize these peaks, second sucrose gradients of the separately pooled fractions corresponding to the 1.05- and 1.08-g/ml peaks were performed. Interestingly, the 1.08-g/ml peak resolved into three antigenic peaks corresponding to the formerly detected ones of 1.05, 1.08, and 1.12 g/ml (Fig. 4). However, the 1.05-g/ml peak stayed as a single identical peak after the second gradient (Fig. 4). Similar data were obtained with all three recombinants. These results suggested that these three peaks could respec-

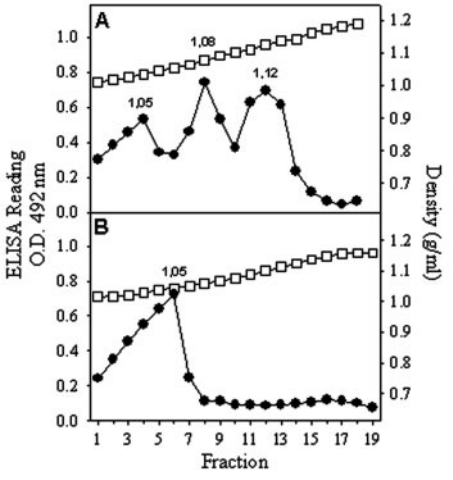

FIG. 4. Second sucrose gradients (0 to 45%) of those fractions corresponding to the 1.08-g/ml (A) and 1.05-g/ml (B) antigenic peaks. Although similar results were obtained with all three recombinants, only data corresponding to the AcNPV-ORF2 baculovirus are shown. Gradient fractions were collected and analyzed as specified in the legend to Fig. 2. O.D., optical density; circles, ELISA readings; squares, density.

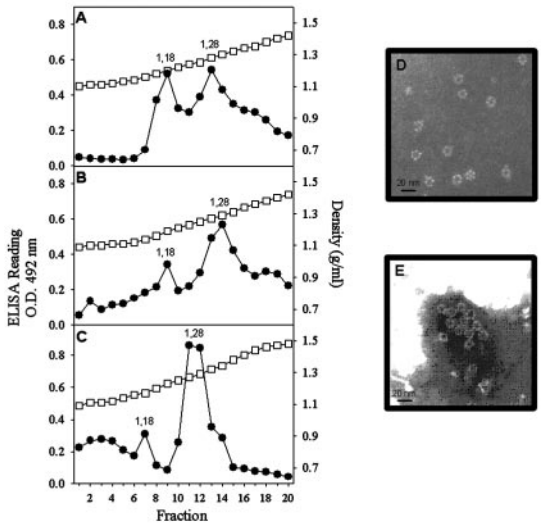

FIG. 5. CsCl-TNE gradients (0 to 50%) of soluble fractions obtained after cell lysis. (A) AcNPV-ORF2; (B) AcNPV-ΔORF2; (C) AcNPV-GFPΔORF2. Gradient fractions were collected and analyzed as specified in the legend to Fig. 2. (D) Electron micrograph of the 1.28-g/ml antigenic peak of the AcNPV-ORF2 construct. (E) Immunoelectron microscopy of the antigenic peak of the AcNPV-ORF2 construct with the polyclonal anti-HAstV-1 antibody. O.D., optical density; circles, ELISA readings; squares, density.

tively correspond to soluble proteins, to an intermediate capsomer-like structure or to T=1, and to T=3 VLPs.

In vitro disassembly and reassembly of VLPs. To evaluate the role of the ring-like structures in the morphogenesis of astrovirus VLPs, a series of disassembly and reassembly experiments were undertaken. Since it has been previously described that divalent cations are needed to stabilize astrovirus particles (22), the addition of a chelating agent, such as EDTA, was tested as a disassembling factor in the purification. Surprisingly, when TN buffer was replaced by TNE buffer in the CsCl gradients, two antigenic peaks of 1.18 and 1.28 g/ml instead of the single peak of 1.28 g/ml were detected with all of the recombinant products (Fig. 5). Electron microscopy observations of both peaks revealed the replacement of VLPs by ring-like structures of 16 nm in the 1.28-g/ml peak (Fig. 5) and the complete absence of structured material in the new 1.18-g/ml peak. The astroviral nature of these structures was confirmed by immunoelectron microscopy (Fig. 5) with the polyclonal anti-HAstV-1 antibody. To promote the reassembly of these ring-like structures, a dialysis treatment against TNMg buffer was conducted to remove the EDTA and to add Mg^{2+} ions. When these treated suspensions were evaluated by electron microscopy, the replacement of the ring-like structures by complete VLPs was observed (Fig. 6). Additionally both kinds of suspensions, ring-like structures and reconstituted VLPs, were loaded onto sucrose gradients and separated as described before. The ring-like structures evolved as two peaks with densities of 1.05 and 1.08 g/ml (Fig. 6). The reconstituted VLPs also evolved in two antigenic peaks, with the first corresponding to that of soluble proteins (1.05 g/ml) and the second corresponding to that of actual VLPs (1.12 g/ml) (Fig. 6).

To determine if the same kind of ring-like structures could also be generated from the actual astrovirus particles, parallel disassembly experiments were conducted with HAstV-1 stocks. In this case, the 1.34-g/ml CsCl peak corresponding to the infectious viruses disappeared while the 1.28-g/ml peak was maintained and the 1.18-g/ml peak appeared again (Fig. 7). Ring-like structures of 16 nm were also observed in the 1.28-g/ml peak (Fig. 7).

Antigenic and biochemical characterization of VLPs and ring-like structures. The immunological recognition of both structures, VLPs and ring-like structures, by two MAbs was assayed. All three kinds of VLPs and ring-like structures reacted equally well with MAb 8E7 (Table 1). Interestingly, however, a significantly higher recognition of ring-like structures was detected with MAb 5B7 (Table 1).

The protein composition of these structures, before and

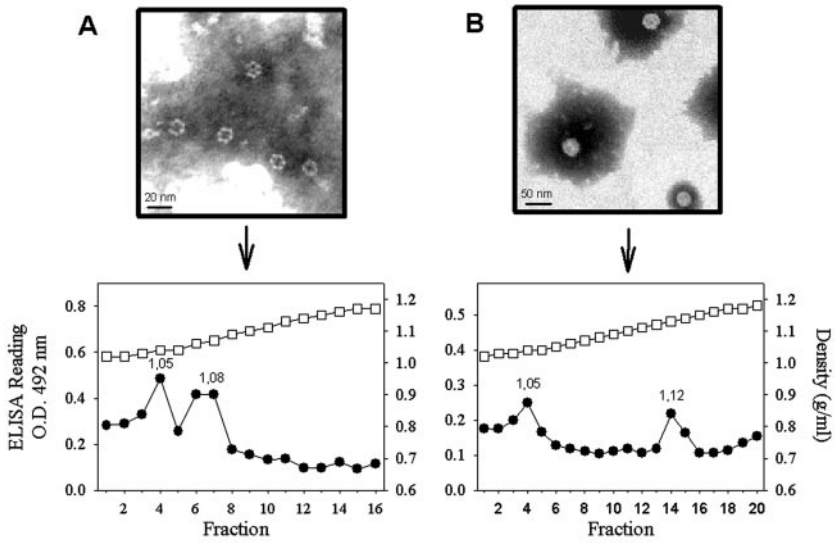

FIG. 6. Sucrose gradients (0 to 45%) of ring-like structures (A) and reconstituted VLPs (B) of the AcNPV-ORF2 construct. Gradient fractions were collected and analyzed as specified in the legend to Fig. 2. O.D., optical density; circles, ELISA readings; squares, density.

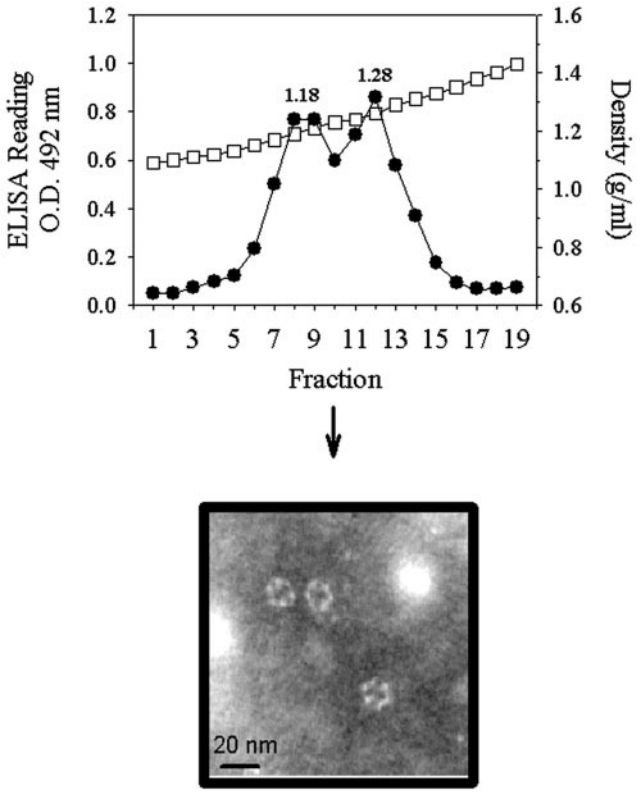

FIG. 7. CsCl gradients (0 to 50%) of HAsVt-1 stocks in TNE buffer. Gradient fractions were collected and analyzed as specified in the legend to Fig. 2. O.D., optical density; circles, ELISA readings; squares, density.

after trypsin treatment, was evaluated. After a concentration step of the structures by immunoprecipitation, proteins were revealed by Western blotting (data not shown). Before trypsin treatment, ring-like structures were composed of the same single proteins described above for VLPs. As expected, after trypsin treatment, two bands of around 34 and 26 kDa were observed in both VLPs and ring-like structures from the complete construct. In contrast, only the band of 26 kDa was clearly revealed with the other two constructs. This result is coherent in the case of the ΔORF2 construct, since the truncated form of the 34-kDa band is equivalent to 26 kDa. In the case of the GFPΔORF2 construct, the expected band of around 57 kDa could not be detected due to its molecular mass coincidence with that of the heavy chains of immunoglobulins, also detected by an immunoprecipitation and Western blot method.

TABLE 1. MAb recognition of VLPs and ring-like structures from the different astrovirus constructs

Construct	Structure	Recognition (mean ± SD) of MAb:	
		8E7	5B7
AcNPV-ORF2	VLP	1.232 ± 0.062	0.616 ± 0.013
AcNPV-ORF2	Ring-like	1.246 ± 0.142	1.254 ± 0.092
AcNPV-ΔORF2	VLP	1.247 ± 0.001	0.558 ± 0.001
AcNPV-ΔORF2	Ring-like	1.254 ± 0.139	0.982 ± 0.076
AcNPV-GFPΔORF2	VLP	1.240 ± 0.073	0.620 ± 0.060
AcNPV-GFPΔORF2	Ring-like	1.295 ± 0.065	1.270 ± 0.105
AcNPVRP8		0.235 ± 0.002	0.240 ± 0.004

DISCUSSION

The baculovirus expression system has extensively been used to express capsid protein virus genes and to produce self-assembled VLPs which represent a good tool for the study of viral morphogenesis (7, 11, 15, 17, 39). In the present work, it has been shown that the expression of the full ORF2 of the HAstV-1 genome in the baculovirus expression system leads to the formation of VLPs, as it has been recently described for the vaccinia system (8). However, in our work, the self-assembly of VLPs has also been accomplished from either an amino-terminally truncated form of the ORF2 polyprotein or the same truncated protein in which the removed fragment has been replaced by the GFP protein. In all three cases, the diameter of the VLPs was around 38 nm, in the described range of actual astrovirus virions (20, 32, 37). The astrovirus capsid processing and assembly is still controversial. Recently, three different models have been proposed. In the first model, Bass and Qiu (1) proposed a proteolytic cleavage of the ORF2 polyprotein at its amino terminus, between positions 70 and 71, forming itself into a structural unit. This model was later rejected by several authors who either propose the absence of any cleavage (13) or a cleavage at the carboxy terminus (23), the precise location of which has not been determined. However, our results confirm, regardless of which model is correct, that similar VLPs could be assembled either from the complete 87-kDa polyprotein, the amino-truncated form of 79 kDa, or even with the amino-truncated form fused to the GFP protein of 110 kDa, indicating that the amino terminus is not essential for capsid assembly. A high tolerance to deletions and insertions in the capsid region encompassing aa 11 to 30 has been previously described (13), and to a lesser extent, there is also tolerance in the region from aa 31 to 50 (13). In this latter study, in which several astrovirus mutants were constructed, only data on viral infectivity were reported due to a lack of information on the efficiency of capsid assembly. The VLPs from all three constructs were equally recognized by the polyclonal anti-HAstV-1 antibody and MAbs 8E7 and 5B7, indicating that the first 70 aa of the structural protein may not be essential in the antigen structure. In fact, none of the residues known to be involved in the astrovirus MAb epitopes are located in this region (22).

An interesting morphogenetic finding of the present study was the generation of ring-like structures through the chelation of ions. The results described herein may be interpreted either as being capsomers or T = 1 VLPs, as is the case for similar ring-like structures of Norwalk virus (39). However, while the morphogenesis of Norwalk virus has been studied extensively (31), it is completely unknown in astrovirus. Norwalk virus is composed of a single structural protein (31, 39) that forms homodimers as building blocks in the capsid assembly which could adopt different orientations, resulting in different structures (39). In contrast, the initial building block for astroviruses is unidentified. One possibility, similarly to that of picornaviruses, would be a protomer including three β-barrel domains with a unique orientation corresponding to the properly folded

unprocessed structural protein, with the T = 1 structure not being feasible. However, secondary structure predictions (16) of the astrovirus structural protein reveal the occurrence of only one β-barrel domain, not three, in the VP34 protein (located around positions 72 to 287 of HAstV-1; accession number L23513), which significantly aligns with the VP2 protein of Theiler's murine encephalomyelitis virus, the small coat protein of the bean pod mottle virus, and the S domain of the carnation mottle virus (data not shown), opening the possibility of T = 1 structures. Since the first 70 aa of the structural protein amino terminus are not involved in the predicted β-barrel domain, the assembly of VLPs with the truncated constructs also seems likely. Structural analyses are in progress to further characterize both kinds of structures.

The biochemical characterization revealed an identical protein composition for both types of structures from all of the constructs and an equal susceptibility to trypsin cleavage. The antigenic characterization showed an equal recognition of both rings and VLPs by MAb 8E7 and a significantly higher recognition of ring-like structures by MAb 5B7. The epitope defined by this latter MAb is located in the common part of the VP26 and VP29 proteins (2), and the epitope defined by MAb 8E7 maps around aa 71 to 260 of the VP34 protein (13). These data suggest a different conformation of the VP26 protein in the VLPs and the ring-like structures, making the 5B7 epitope less accessible in the former case.

The role of divalent ions in the stabilization of VLPs is another intriguing issue. While the addition of EDTA to the purification buffers of sucrose gradients does not affect viral stabilization (6, 8), its inclusion in our CsCl buffers completely destabilize VLPs. In fact, the addition of divalent cations (Ca^{2+} and Mg^{2+}) in the purification solutions of CsCl gradients has been found to stabilize viral particles (22). The biological rationale of the role of divalent cations in the astrovirus replication cycle deserves further investigation, since their cytoplasmic concentrations in intestinal cells are very low. A possible explanation could be that, as for rotavirus, this low concentration may be required for the uncoating process (9). Additionally, a higher microenvironment concentration of ions could be expected in membranous compartments, allowing proper capsid assembly. In fact, electron microscopy studies of astrovirus-infected CaCo-2 cells show that the vast majority of particles are included in double-membrane vacuoles (S. Guix, S. Caballero, A. Bosch, and R. M. Pintó, submitted for publication).

ACKNOWLEDGMENTS

S.C. was the recipient of a BRD fellowship from the University of Barcelona.

This study was supported in part by grants QLRT-1999-0634 and QLRT-1999-0594 from the European Union and by 2001/SGR/00098 and the Centre de Biotecnologia de Catalunya (CeRBA) from the Generalitat de Catalunya.

We acknowledge the technical expertise of the Serveis Científic-Tècnics of the University of Barcelona. The authors thank Mary K. Estes and Sue E. Crawford for their advice and useful discussions.

REFERENCES

1. **Bass, D. M., and S. Qiu.** 2000. Proteolytic processing of the astrovirus capsid. J. Virol. **74:**1810–1814.
2. **Bass, D. M., and U. Upadhyayula.** 1997. Characterization of human serotype 1 astrovirus-neutralizing epitopes. J. Virol. **71:**8666–8671.
3. **Belliot, G., H. Laveran, and S. S. Monroe.** 1997. Capsid protein composition of reference strains and wild isolates of human astrovirus. Virus Res. **49:**49–57.
4. **Belliot, G., H. Laveran, and S. S. Monroe.** 1997. Outbreak of gastroenteritis in military recruits associated with serotype 3 astrovirus infection. J. Med. Virol. **51:**101–106.
5. **Bon, F., P. Fascia, M. Dauvergne, D. Tenenbaum, H. Planson, A. M. Petion, P. Pothier, and E. Kohli.** 1999. Prevalence of group A rotavirus, human calicivirus, astrovirus, and adenovirus type 40 and 41 infections among children with acute gastroenteritis in Dijon. J. Clin. Microbiol. **37:**3055–3058.
6. **Caballero, S., S. Guix, W. Morsy El-Senousy, I. Calicó, R. M. Pintó, and A. Bosch.** 2003. Persistent gastroenteritis in astrovirus infected children: association with serotype-3 strains. J. Med. Virol. **71:**245–250.
7. **Crawford, S. E., M. Labbé, J. Cohen, M. H. Burroughs, Y. Zhou, and M. K. Estes.** 1994. Characterization of virus-like particles produced by the expression of rotavirus capsid proteins in insect cells. J. Virol. **68:**5946–5952.
8. **Dalton, R. M., E. P. Pastrana, and A. Sánchez-Fauquier.** 2003. Vaccinia virus recombinant expressing an 87-kilodalton polyprotein that is sufficient to form astrovirus-like particles. J. Virol. **77:**9094–9098.
9. **Estes, M. K.** 2001. Rotavirus and their replication, p. 1747–1785. *In* B. N. Fields, D. M. Knipe, P. M. Howley, D. E. Griffin, M. A. Martin, R. A. Lamb, B. Roizman, and S. E. Straus (ed.), Fields virology. Lippincott Williams & Wilkins, Philadelphia. Pa.
10. **Foley, B., J. O'Mahony, S. M. Morgan, C. Hill, and J. G. Morgan.** 2000. Detection of sporadic cases of Norwalk-like virus (NLV) and astrovirus infection in a single Irish hospital from 1996 to 1998. J. Clin. Virol. **17:**109–117.
11. **French, T. J., and P. Roy.** 1990. Synthesis of bluetongue (BTV) corelike particles by a recombinant baculovirus expressing the two major structural core proteins of BTV. J. Virol. **64:**1530–1536.
12. **Gaggero, A., M. O'Ryan, J. S. Noel, R. I. Glass, S. S. Monroe, N. Mamani, V. Prado, and L. F. Avendaño.** 1998. Prevalence of astrovirus infection among Chilean children with acute gastroenteritis. J. Clin. Microbiol. **36:**3691–3693.
13. **Geigenmüller, U., N. H. Ginzton, and S. M. Matsui.** 2002. Studies on intracellular processing of the capsid protein of human astrovirus serotype 1 in infected cells. J. Gen. Virol. **83:**1691–1695.
14. **Guix, S., S. Caballero, C. Villena, R. Bartolomé, C. Latorre, N. Rabella, M. Simó, A. Bosch, and R. M. Pintó.** 2002. Molecular epidemiology of astrovirus infection in Barcelona, Spain. J. Clin. Microbiol. **40:**133–139.
15. **Jiang, X., M. Wang, D. Y. Graham, and M. K. Estes.** 1992. Expression, self-assembly, and antigenicity of the Norwalk virus capsid protein. J. Virol. **66:**6527–6532.
16. **Kelley, L. A., R. M. MacCallum, and M. J. E. Sternberg.** 2000. Enhanced genome annotation using structural profiles in the program 3D-PSSM. J. Mol. Biol. **299:**499–520.
17. **Kosukegawa, A., F. Arisaka, M. Takayama, H. Yahima, A. Kaidow, and H. Handa.** 1996. Purification and characterization of virus-like particles and pentamers produced by the expression of SV40 capsid proteins in insect cells. Biochim. Biophys. Acta **1920:**37–45.
18. **Lee, T. W., and J. B. Kurtz.** 1994. Prevalence of human astrovirus serotypes in the Oxford region 1976–92, with evidence for two new serotypes. Epidemiol. Infect. **112:**187–193.
19. **Lewis, T. L., and S. M. Matsui.** 1996. Astrovirus ribosomal frameshifting in an infection-transfection transient expression system. J. Virol. **70:**2869–2875.
20. **Madeley, C. R., and B. P. Cosgrove.** 1975. 28 nm particles in faeces in infantile gastroenteritis. Lancet **ii:**451–452.
21. **Marczinke, B., A. J. Bloys, T. D. Brown, M. M. Willcocks, J. M. Carter, and I. Brierley.** 1994. The human astrovirus RNA-dependent RNA polymerase coding region is expressed by ribosomal frameshifting. J. Virol. **68:**5588–5595.
22. **Matsui, S. M., and H. B. Greenberg.** 2001. Astroviruses, p. 875–893. *In* B. N. Fields, D. M. Knipe, P. M. Howley, D. E. Griffin, M. A. Martin, R. A. Lamb, B. Roizman, and S. E. Straus (ed.), Fields virology. Lippincott Williams & Wilkins, Philadelphia. Pa.
23. **Méndez, E., T. Fernández-Luna, S. López, M. Méndez-Toss, and C. F. Arias.** 2002. Proteolytic processing of a serotype 8 human astrovirus ORF2 polyprotein. J. Virol. **76:**7996–8002.
24. **Mitchell, D. K., S. S. Monroe, X. Jiang, D. O. Matson, R. I. Glass, and L. K. Pickering.** 1995. Virologic features of an astrovirus diarrhea outbreak in a day care center revealed by reverse transcriptase-polymerase chain reaction. J. Infect. Dis. **172:**1437–1444.
25. **Monroe, S. S., B. Jiang, S. E. Stine, M. Koopmans, and R. I. Glass.** 1993. Subgenomic RNA sequence of human astrovirus supports classification of *Astroviridae* as a new family of RNA viruses. J. Virol. **67:**3611–3614.
26. **Monroe, S. S., S. E. Stine, L. Gorelkin, J. Herrmann, N. R. Blacklow, and R. I. Glass.** 1991. Temporal synthesis of proteins and RNAs during human astrovirus infection of cultured cells. J. Virol. **67:**641–648.
27. **Mustafa, H., E. A. Palombo, and R. F. Bishop.** 2000. Epidemiology of astrovirus infection in young children hospitalized with acute gastroenteritis in Melbourne, Australia, over a period of four consecutive years, 1995 to 1998. J. Clin. Microbiol. **38:**1058–1062.

28. **Noel, D., and D. Cubbit.** 1994. Identification of astrovirus serotypes from children treated at the Hospitals for Sick Children, London 1981–93. Epidemiol. Infect. **113:**153–159.
29. **Oishi, I., K. Yamazaki, T. Kimoto, Y. Minekawa, E. Utagawa, S. Yamazaki, S. Inouye, G. S. Grohmann, S. S. Monroe, S. E. Stine, C. Carcano, T. Ando, and R. I. Glass.** 2000. A large outbreak of acute gastroenteritis associated with astrovirus among students and teachers in Osaka, Japan. J. Infect. Dis. **170:**439–443.
30. **Pintó, R. M., J. M. Diez, and A. Bosch.** 1994. Use of the colonic carcinoma cell line CaCo-2 for in vivo amplification and detection of enteric viruses. J. Med. Virol. **44:**310–315.
31. **Prasad, B. V. V., R. Rothnagel, X. I. Jiang, and M. K. Estes.** 1994. Three-dimensional structure of baculovirus-expressed norwalk virus capsids. J. Virol. **68:**5117–5125.
32. **Risco, C., J. L. Carrascosa, A. M. Pedregosa, C. D. Humphrey, and A. Sánchez-Fauquier.** 1995. Ultrastructure of human astrovirus serotype 2. J. Gen. Virol. **76:**2075–2080.
33. **Sakamoto, T., H. Negishi, Q. Wang, S. Akihara, B. Kim, S. Nishimura, K. Kaneshi, S. Nakaya, Y. Ueda, K. Sugita, T. Motohiro, T. Nishimura, and H. Ushijima.** 2000. Molecular epidemiology of astrovirus in Japan from 1995 to 1998 by reverse transcription-polymerase chain reaction with serotype-specific primers (1 to 8). J. Med. Virol. **61:**326–331.
34. **Svenungsson, B., A. Lagergren, E. Ekwall, B. Evengard, K. O. Hedlund, A. Kärnell, S. Lörfdahl, L. Svensson, and A. Weintraub.** 2000. Enteropathogens in adult patients with diarrhea and healthy control subjects: a 1-year prospective study in a Swedish clinic for infectious diseases. Clin. Infect. Dis. **30:**770–779.
35. **Taylor, M. B., F. E. Marx, and W. O. K. Grabow.** 1997. Rotavirus, astrovirus and adenovirus associated with an outbreak of gastroenteritis in a South African child care centre. Epidemiol. Infect. **119:**227–230.
36. **Unicomb, L. E., N. N. Banu, T. Azim, A. Islam, P. K. Bardhan, A. S. G. Faruque, A. Hall, C. L. Moe, J. S. Noel, S. S. Monroe, M. J. Albert, and R. I. Glass.** 1998. Astrovirus infection in association with acute, persistent and nosocomial diarrhea in Bangladesh. Pediatr. Infect. Dis. J. **17:**611–614.
37. **van Regenmortel, M. H. V., C. M. Fauquet, D. H. L. Bishop, E. B. Carstens, M. K. Estes, S. M. Lemon, J. Manilov, M. A. Mayo, D. J. McGeoch, C. R. Pringle, and R. B. Wickner (ed.).** 2000. Virus taxonomy, p. 1162. Academic Press, San Diego, Calif.
38. **Walter, J. E., and D. K. Mitchell.** 2000. Role of astrovirus in childhood diarrhea. Curr. Opin. Pediatr. **12:**275–279.
39. **White, L. J., M. E. Hardy, and M. K. Estes.** 1997. Biochemical characterization of a smaller form of recombinant Norwalk virus capsids assembled in insect cells. J. Virol. **71:**8066–8072.
40. **Willcocks, M. M., M. J. Carter, F. R. Laidler, and C. R. Madeley.** 1990. Growth and characterisation of human faecal astrovirus in a continuous cell line. Arch. Virol. **113:**73–81.